Manuscript Details

Manuscript number	ENVPOL_2017_2217_R2
Title	Assessment of light extinction at a European polluted urban area during wintertime: Impact of PM1 composition and sources
Article type	Research Paper

Abstract

In this paper, results from receptor modelling performed on a well-characterised PM1 dataset were combined to chemical/reconstructed light extinction data (bext) with the aim of assessing the impact of different PM1 components and sources on light extinction and visibility at a European polluted urban area. It is noteworthy that, at the state of the art, there are still very few papers estimating the impact of different emission sources on light extinction as we present here, although being among the major environmental challenges at many polluted areas. Following the concept of the well-known IMPROVE algorithm, here a tailored site-specific approach (recently developed by our group) was applied to assess chemical light extinction due to PM1 components and major sources. PM1 samples collected separately during daytime and nighttime at the urban area of Milan (Italy) were chemically characterised for elements, major ions, elemental and organic carbon, and levoglucosan. Chemical light extinction was estimated and results showed that at the investigated urban site it is heavily impacted by ammonium nitrate and organic matter. Receptor modelling (i.e. Positive Matrix Factorization, EPA-PMF 5.0) was effective to obtain source apportionment; the most reliable solution was found with 7 factors which were tentatively assigned to nitrates, sulphates, wood burning, traffic, industry, fine dust, and a Pb-rich source. The apportionment of aerosol light extinction (bext,aer) according to resolved sources showed that considering all samples together nitrate contributed at most (on average 41.6%), followed by sulphate, traffic, and wood burning accounting for 18.3%, 17.8% and 12.4%, respectively.

Keywords	PM1, light extinction, composition, sources

Corresponding Author	Roberta Vecchi
Corresponding Author's Institution	Dept. of Physics Università degli Studi di Milano
Order of Authors	Roberta Vecchi, Vera Bernardoni, Sara Valentini, Gianluigi Valli, Andrea Piazzalunga, PAOLA FERMO

Suggested reviewers	Fumo Yang, Giovanni Lonati, Xinghua Li, Imre SALMA, Junji Cao

Submission Files Included in this PDF

File Name [File Type]

letter_ENVPOLL_rev2.pdf [Cover Letter]

response to reviewers_REV2.pdf [Response to Reviewers]

Vecchi_ENVPOLL_REV2-tracked.doc [Revised Manuscript with Changes Marked]

Highlights_REV.docx [Highlights]

graphical abstract_rev.pdf [Graphical Abstract]

Vecchi_ENVPOLL_REV2.doc [Manuscript File]

Figure1_REV.pdf [Figure]

Figure2_REV.pdf [Figure]

Figure3_REV.pdf [Figure]

Figure4_REV.pdf [Figure]

Figure5_REV.pdf [Figure]

Supplementary Material_REV2.pdf [Supporting File]

To view all the submission files, including those not included in the PDF, click on the manuscript title on your EVISE Homepage, then click 'Download zip file'.

Assessment of light extinction at a European polluted urban area during wintertime: Impact of PM1 composition and sources

R. Vecchi[1,*], V. Bernardoni[1], S. Valentini[1], G. Valli[1], A. Piazzalunga[2,3], and P. Fermo[2]

[1]Department of Physics, Università degli Studi di Milano and INFN Milan, Italy

[2] Department of Chemistry, Università degli Studi di Milano, Milano, Italy

[3] now at: Water & Life Lab srl, Entratico, Bergamo, Italy

*Corresponding Author:
Prof. Roberta Vecchi
Department of Physics
Università degli Studi di Milano
Via Celoria 16
20133 Milan
Italy
tel: +39 02 50317498
email: roberta.vecchi@unimi.it

Abstract

In this paper, results from receptor modelling performed on a well-characterised PM1 dataset were combined to chemical/reconstructed light extinction data (b_{ext}) with the aim of assessing the impact of different PM1 components and sources on light extinction and visibility at a European polluted urban area. It is noteworthy that, at the state of the art, there are still very few papers estimating the impact of different emission sources on light extinction as we present here, although being among the major environmental challenges at many polluted areas. Following the concept of the well-known IMPROVE algorithm, here a tailored site-specific approach (recently developed by our group) was applied to assess chemical light extinction due to PM1 components and major sources.

PM1 samples collected separately during daytime and nighttime at the urban area of Milan (Italy) were chemically characterised for elements, major ions, elemental and organic carbon, and levoglucosan. Chemical light extinction was estimated and results showed that at the investigated urban site it is heavily impacted by ammonium nitrate and organic matter. Receptor modelling (i.e. Positive Matrix Factorization, EPA-PMF 5.0) was effective to obtain source apportionment; the most reliable solution was found with 7 factors which were tentatively assigned to nitrates,

sulphates, wood burning, traffic, industry, fine dust, and a Pb-rich source. The apportionment of aerosol light extinction ($b_{ext,aer}$) according to resolved sources showed that considering all samples together nitrate contributed at most (on average 41.6%), followed by sulphate, traffic, and wood burning accounting for 18.3%, 17.8% and 12.4%, respectively.

Capsule: Chemical light extinction at an urban site was assessed using tailored extinction coefficients and the role of major PM1 components and sources was estimated.

Keywords: PM1, light extinction, composition, sources

1. Introduction

In the last decades, the concern for particulate matter (PM) fine fractions increased due to their adverse effects on human health, climate and visibility. Air pollution impacts on solar light extinction; this is a parameter which can be related to visibility as routinely done by the Interagency Monitoring of Protected Visual Environments (IMPROVE) network in the US (Malm et al., 1994; Pitchford et al., 2007; Watson, 2002). Visibility impairment results from a combination of light scattering and absorption by both gases and aerosols but poor visibility at urban sites is mainly attributed to fine particles.

From the scientific and legislative point of view, studies on particulate matter moved from PM10 (EU Air Quality Directive EC/30/1999 and EN12341) to PM2.5 (EN14907/2005) and, more recently, the scientific community has addressed its interest to sub-micron sized (PM1, aerodynamic diameter lower than 1 μm) and ultrafine particles (UFP, aerodynamic diameter lower than 0.1 μm) as smaller sized aerosols can penetrate deeply into the respiratory system causing adverse health effects (e.g. Corsini et al., 2017; Heinzerling et al., 2016).

At different locations in Europe, PM1 can be a significant fraction of PM2.5 and PM10 (e.g. Rogula-Kozłowska and Keljnowski, 2013; Theodosi et al., 2011; Vecchi et al., 2008a) and previous studies demonstrated that it can be considered a good indicator of emissions from anthropogenic sources (e.g. Pérez et al., 2008; Perrone et al. 2013).

Few previous studies on PM1 physical-chemical properties and sources were performed in Milan (Giugliano et al., 2005; Putaud et al., 2002; Vecchi et al., 2004; Vecchi et al., 2008a). Notwithstanding, none of them investigated daytime and nighttime PM1 concentrations, composition, sources, and their impact on light extinction as done in this work for wintertime, i.e. the period of the year when Milan typically experiences very high PM concentrations. At heavily polluted areas such as the Po valley and the large urban sites located there, air quality management

policy and risk assessment need a comprehensive knowledge of the detrimental pollutants as well of major emission sources.

The straightforward way to assess light extinction is based on direct measurements of aerosol optical properties (i.e. extinction, scattering, and absorption coefficients) using dedicated instrumentation. Unfortunately, these instruments (e.g. nephelometers, absorption/extinction analysers) are not always available in monitoring networks or during measurement campaigns thus preventing any information about visibility and aerosol optical properties. In this frame, the alternative and simple approach proposed by the IMPROVE algorithm, giving estimates of the extinction coefficient through chemical components assessment, can be very useful although less accurate. Indeed, in many monitoring networks and measurement campaigns PM samples are routinely collected and chemically analysed for retrieving aerosol composition; these data can be fruitfully used also to estimate light extinction as done in the IMPROVE network.

In this paper, to assess atmospheric light extinction and visibility impairment a tailored site-specific approach (recently developed by our group; for details see Valentini et al., accepted for publication) is used to better exploit the characteristics of the well-known IMPROVE algorithm as explained in section 2.3. It is noteworthy that the application of the IMPROVE algorithm (both the original and the revised version) is increasing at highly polluted sites in China (e.g. Cao et al., 2012; Tao et al., 2014; Wang et al., 2015a,b; Wang et al., 2016).

At the state of the art, there are still very few papers (e.g. Eatough and Farber, 2009; Cao et al., 2012; Chen et al., 2014; Xiao et al., 2014; Wang et al., 2016) estimating the impact of the different emission sources on light extinction (i.e. chemical light extinction, b_{ext}) and visibility as we present in this paper, although being among the major environmental challenges at many polluted areas. In addition, as far as we know, this is the first time that the contribution to light extinction due to different aerosol components and sources was assessed at a European pollution hot spot site.

2. Material and Methods

2.1 The measurement campaign

PM1 aerosol measurements were performed in Milan (45°27’ N, 9°11’ E) which is the largest town in the Po valley (Italy) (a map is given in Figure S1, Supplementary Material); the latter is a renown pollution hot-spot in Europe characterised by low atmospheric dispersion especially during wintertime.

The sampling campaign was carried out at our urban background monitoring station, at about 10 meters a.g.l. in the University campus (details about the site in Vecchi et al., 2009) during

wintertime 2012 (from 9th January to 18th March). It was stopped from 6th to 14th February because of instruments failure due to very low temperatures (minimum T at -5.9°C).

PM1 samples were collected in parallel on quartz-fibre (Pall, 2500 QAO-UP, 47mm diameter) and PTFE (Whatman, PM2.5 Membranes, 46.2 mm with ring) filters using low-volume sequential samplers (Charlie HV coupled to Sentinel PM by TCR Tecora srl-Italy; and LVS 3 by Derenda-Germany) operated at a 2.3 m^3/h flow-rate. Nighttime and daytime 9-hours samplings (07-16; 19-04 local time, LT) were performed collecting 120 samples in total. Shortened time slots were needed to avoid filter clogging and were chosen in order to sample during major emission periods (e.g. traffic rush hours and wood burning hours for domestic heating in the evening).

Before and after the sampling, filters were conditioned for 48 hours in an air-controlled weighing room (T = 20 ±1 °C and R.H. = 50 ± 5 %). PM1 mass concentration was determined by weighing them using an analytical microbalance (precision 1 μg, details in Vecchi et al., 2004).

Samples were chemically characterised as follows: elements by Energy Dispersive X-Ray Fluorescence analysis on PTFE filters (ED-XRF, details in Vecchi et al. 2004), ions by Ionic Chromatography on a portion of each quartz-fibre filter (IC, details in Piazzalunga et al., 2013), elemental and organic carbon (EC and OC) by thermal optical transmittance analysis on a punch taken from each quartz-fibre filter (TOT using NIOSH-like thermal protocol, details in Piazzalunga et al., 2013), anhydrosugars by high performance anion-exchange chromatography coupled with pulsed amperometric detection on a portion of each quartz-fibre filter (HPAEC-PAD, details in Piazzalunga et al., 2010).

Moreover, to retrieve the light-absorption coefficient at 635 nm the samples were analysed using a polar photometer (PP_UniMI, details in Vecchi et al. 2014).

Equivalent black carbon (EBC) concentrations were monitored during the winter campaign in 2012 by a Multi Angle Absorption Photometer (MAAP, Thermo Scientific) operated with a 5-min resolution and equipped with a PM1 inlet. To obtain the most reliable equivalent black carbon concentrations (Petzold et al., 2013), MAAP data were corrected using a campaign-specific mass absorption coefficient (MAC) which resulted to be 11.6 m^2/g. This value was retrieved from the aerosol absorption coefficient value (b_{abs} in Mm^{-1}) measured on every quartz-fibre filter by our polar photometer and the EC concentration measured by thermal-optical analysis on the same filter (Figure S2 in the Supplementary Material). It is worthy to note that raw MAAP data were corrected following the approach described in Hyvärinen et al. (2013).

Ancillary measurements were available: particle number concentration and size distributions were retrieved by a Scanning Mobility Particle Sizer (31 size bins, 8-700 nm, details in Bigi and Ghermandi, 2011) and an Optical Particle Counter (Grimm, OPC model 1.107, 31 size bins, 0.25-

32 µm, see Mazzei et al., 2007 for details). Moreover, ^{222}Rn 1h-resolution concentrations for evaluating atmospheric stability conditions (details in Marcazzan et al. 2003), meteorological parameters (temperature, pressure, relative humidity, wind speed and direction, global solar radiation, precipitation) recorded by the meteorological station located at the same urban background monitoring station, and gaseous pollutants data retrieved by the nearby station of the Environmental Agency of Lombardy (www.arpalombardia.it) were used for data interpretation.

2.2 Receptor modelling for source apportionment and light extinction source apportionment

Positive Matrix Factorization (PMF) was the receptor model used in this work. It is a least squares program for solving multi-linear problems. Specifically, it solves models where the data values are fitted by sums of products of unknown factor elements (Paatero, 2000). For bilinear problems it takes the form X = G•F + E, where X is the known n by m matrix of the m measured chemical species in n samples; G is an n by p matrix of factor contributions to the samples; F is a p by m matrix of species concentrations in the factor profile; p is the factors number. G and F are factor matrices to be determined and they are constrained to non-negative values only. E is defined as a residual matrix i.e. the difference between the measurements X and the model Y = G•F as a function of G and F.

The dataset was analysed with EPA-PMF 5.0 (Norris et al., 2014) and comprised only strong variables, defined according to the signal-to-noise criterion reported in Paatero (2015). All data were pre-treated according to Polissar et al. (1998) as for uncertainties, below detection limits, and missing data.

The optimal solution for the base case was given by 7 factors (tentatively assigned to nitrate, sulphate, wood burning, traffic, industry, fine dust, and a Pb-rich source; see section 3.3 for details) obtaining a Q_{true}/Q_{robust}=1.0 with residues comprised in the ±3 interval (only 5 cases out of 109 were slightly larger than ±3). The modelled PM1 mass concentration reconstructed the measured PM1 mass very well (R^2=0.96, slope=0.98 intercept=-33 ng/m^3, i.e. intercept compatible with zero). Also the various PM components were generally fairly reconstructed ($0.60<R^2<0.99$), with the only exception of Ti (R^2=0.16) - whose regression data showed a large dispersion likely due to frequent values near or below to minimum detection limits - and to a less extent Br (R^2=0.56).

It is worthy to note that the 6-factor solution still showed the Pb-rich source; furthermore, the traffic and industry factors were somehow mixed. The choice to keep the 7-factor solution was done after evaluating results from the bootstrap analysis, which gave a lower number of unmapped cases (i.e. 8% at maximum). Also rotational ambiguity was explored by Fpeak changes and the most meaningful physical solution resulted the one with Fpeak=0.5. Indeed, the latter solution showed

much clearer chemical profiles and higher percentages for tracer components. Also in this case, the bootstrap analysis (100 runs) was the parameter that drove toward the final solution as the unmapped cases for each factor were less than in the base case (i.e. 1% at maximum).

The apportionment of aerosol light extinction according to resolved sources, gave information about which source emissions caused the largest visibility impairment. In this work, a multi-linear regression analysis was applied to the sources resolved by PMF (i.e. elements of the G matrix) and $b_{ext,aer}$ (i.e. considering only the contribution to b_{ext} due to aerosol components thus excluding Rayleigh scattering and NO_2 contributions) to assess source contributions to $b_{ext,aer}$.

2.3 Calculation of chemical extinction coefficient by a tailored approach

Following the IMPROVE algorithm (Malm et al., 1994; Pitchford et al., 2007; Watson, 2002), the light extinction coefficient (b_{ext} in Mm^{-1}) for the atmosphere can be simply expressed as the sum of PM scattering (b_{sp}), PM absorption (b_{ap}), pollutant gases absorption (mainly NO_2, b_{ag}) and Rayleigh clear-air scattering (b_{sg}). The original IMPROVE equation was revised by Pitchford et al. in 2007 to account for some biases and specific coefficients for the small and large mode – accounting for fresh and aged aerosol – were implemented (so that the IMPROVE revised algorithm is also called split-component model). It is noteworthy that the application of the latter model requires the use of an empirical factor to split the PM components in small and large fractions. As it was developed for U.S. monitoring sites and never checked at highly polluted locations with different PM characteristics like the Po valley sites, the IMPROVE approach was modified by Valentini et al. (accepted for publication) tailoring it for our monitoring site, in order to reduce possible additional uncertainties in light extinction estimates. The chemical extinction equation used in this work was:

$$b_{ext} = c_1 \cdot f_1(RH) \cdot [ammonium\ sulphate] + c_2 \cdot f_2(RH) \cdot [ammonium\ nitrate] + c_3 \cdot f_3(RH) \cdot [organic\ matter] + c_4 \cdot [fine\ soil] + b_{ap} + 0.60 \cdot [coarse\ mass] + 0.33 \cdot [NO_2]\ (ppb) + Rayleigh\ scattering$$

Concentrations of the various components are reported in square brackets. Site-specific extinction efficiencies (c_1-c_4) calculated from aerosol size distributions recorded in Milan instead of those reported in the IMPROVE algorithm were used. Indeed, size-segregated sampling was running in parallel to PM1 collection so that experimental data for mass, major ions, elements, and carbon components size distributions were available (data reported in Bernardoni et al., 2017; Elser Fritsche, 2012). The detailed procedure for compound-specific extinction efficiency calculation is described in Valentini (2016) and Valentini et al. (accepted for publication); basically, they were retrieved from size distribution measurements of every chemical component of interest and using the discrete dipole approximation code (ADDA) to simulate light scattering from atmospheric particles. As done in the IMPROVE approach, particles are assumed to be externally mixed

(although it is well known that they could be internally mixed, see e.g. Li et al., 2016). The multiplying efficiencies inserted in the tailored equation by Valentini et al., (accepted for publication) were thus as follows: c_1=4.4; c_2=5.2; c_3=6.1; c_4=3.2. The efficiencies for NO_2 and coarse mass were taken from Watson (2002). The hygroscopic growth functions $f_{1,2,3}$(RH) were calculated for every sample considering ambient relative humidity values. Opposite to the IMPROVE algorithm, they were retrieved separately for ammonium sulphate, ammonium nitrate, and organic matter in order to avoid further assumptions; indeed, in the IMPROVE algorithm no f(RH) is considered for OM and f(RH) curves for ammonium sulphate are also applied to ammonium nitrate. Due to the availability of light absorption measurements performed on the same samples (Vecchi et al., 2014) and because of the inaccuracy in the determination of the extinction coefficient for EC reported by Valentini et al. (accepted for publication), b_{ap} was directly inserted in the equation instead of using elemental carbon concentrations and calculated extinction efficiency for this component. As extinction efficiencies are typically calculated at 550 nm, also b_{ap} was recalculated at the same wavelength using an Ångström Absorption Coefficient of 1.

Organic mass (OM) was estimated from OC concentration using a conversion factor of 1.6 (see also section 3.1), fine soil was calculated using the formula reported in Marcazzan et al. (2001) and the coarse mass in this work was considered as the difference between PM10 and PM1 concentrations. The clear-sky Rayleigh scattering efficiency (in Mm^{-1}) was calculated as in Watson (2002) using atmospheric temperature and pressure data collected at our monitoring station; likewise, the absorption contribution due to atmospheric gases (mainly NO_2) was evaluated from concentrations recorded in Milan by the regional monitoring network (ARPA Lombardia) during the sampling period. Sea salt contribution was neglected as not detected in PM1 in Milan.

3. Results and discussion

3.1 PM1 mass concentration and composition

In Table 1 mass concentration (in $\mu g/m^3$) and relative contributions (in %) of PM1 components (i.e. fine soil, heavy metal oxides, organic matter, elemental carbon, nitrate, sulphate, and ammonium) are reported for the whole campaign and separately for daytime (07-16 LT) and nighttime (19-04 LT). In addition, in Table S1 (Supplementary Material) a basic statistics on chemical species (in ng/m^3) concentration detected in PM1 is given.

Median daytime and nighttime PM1 mass concentrations differed only slightly (i.e. 31.0 $\mu g/m^3$ and 33.0 $\mu g/m^3$ were the daytime and nighttime median values, respectively) as expected due to the relatively high residence times of fine particles. Indeed, applying the methodology published in Vecchi et al. (2005) average residence time for fine particles was estimated to be 37±8 hours in

238 Milan during winter 2012 (Crova, 2017). The mass closure - performed following Vecchi et al.
239 (2008a) - showed that the unaccounted fraction was on average about 12% of PM1 mass and could
240 be likely due to atmospheric water uptake by hygroscopic PM compounds. Anions and cations
241 contents were well balanced within 8%.
242 In the Po valley there is a large availability of ammonia making it one of the large hot-spots for
243 ammonia emissions in Europe as reported in the literature (e.g. Carozzi et al., 2012; EAA, 2011;
244 Van Damme et al., 2016). Therefore, nitrates and sulphates are typically in the form of ammonium
245 nitrate and ammonium sulphate. The most relevant contributions were due to organic matter and
246 ammonium nitrate explaining together on average 68% of the PM1 mass. Organic matter and
247 ammonium nitrate concentrations accounted for about 12 and 15 $\mu g/m^3$, respectively (Figure 1)
248 with the water-soluble OC fraction explaining nearly 74% of total OC (data not shown), which was
249 in the range of values reported by other authors (e.g. Jaffrezo et al., 2005). In particular, ammonium
250 nitrate dominated when high pollution events occurred in Milan (i.e. when PM10 and PM2.5 EU
251 thresholds are largely exceeded), contributing for more than half of the PM1 mass; during these
252 heavily polluted days ammonium nitrate reached concentrations up to 67 $\mu g/m^3$ and PM1 mass
253 concentration was as high as 113 $\mu g/m^3$. It is noteworthy that huge ammonium nitrate peaks were
254 also observed in PM10 during a previous campaign in Milan carried out in 2007 by our group
255 (Vecchi et al., 2008b, see Figure S3 in the Supplementary Material) as well as by Poluzzi et al.
256 (2013) at other sites in the Po valley (Northern Italy) during the same period as the campaign here
257 described. This nitrate peak might have been triggered by a sudden availability of ammonia for
258 agricultural fields manure as regional laws ban the use of nitrogen fertilizers from livestocks (in
259 Lombardy the livestock loading exceeds 6.2 millions units) from mid November to mid February.
260 This is an issue that has been not fully investigated yet in the Po valley.
261 The so-called EC tracer method (Turpin and Huntzicker, 1995) was applied to give a rough estimate
262 of primary and secondary OC contributions. In this work, $(OC/EC)_{min} = 1.2$ was obtained regressing
263 OC vs EC values only for OC-to-EC ratios lower than the fifth percentile, as this was considered to
264 be the best estimate for samples mostly impacted by primary emissions. The median secondary OC
265 contribution (OC_{sec}) was estimated to be 54% of total OC. The overall median contribution to PM1
266 mass due to secondary aerosol – evaluated as the sum of ammonium nitrate, ammonium sulphate
267 and secondary organic matter – was notably high, i.e. 63%.
268 At urban sites like Milan where PM levels are exceeded, traffic and wood burning are the major
269 sources often considered responsible of poor air quality (e.g. EEA, 2016).
270 In Reche et al. (2011), the monitoring of black carbon concentrations at urban sites was reported as
271 a suitable proxy for exhaust traffic emissions and this indication was also given in the EEA

Technical report No 18/2013. In Milan, Invernizzi et al. (2011) successfully demonstrated that black carbon was a proper metric to assess pollutant reduction in traffic-restricted areas. In this work, the equivalent black carbon (EBC) median value was 2.4 $\mu g/m^3$ ranging from 0.8 to 7.4 $\mu g/m^3$ (10^{th} and 90^{th} percentile, respectively). The EBC median daytime (2.8 $\mu g/m^3$) vs. nighttime (3.0 $\mu g/m^3$) concentrations did not show significant differences; furthermore, the EBC and ^{222}Rn concentration patterns were fairly similar (Figure 2) suggesting that the mixing layer height played an important role in EBC temporal evolution.

Similar daily modulation was shown by EBC, particle number (total number concentration for particles smaller than 700 nm) and NO_x concentrations (Figure 3a). The role of the atmospheric stability on highest pollution levels and the dispersion conditions in the afternoon on lowest ones were also evident from the diurnal pattern of ^{222}Rn concentration reported in the same figure, where typically the highest ^{222}Rn concentrations were observed in early morning (corresponding to shallow mixing layer heights) and the lowest in mid-afternoon (corresponding to high mixing layer heights). Indeed, high radon levels typically indicate poor dispersion conditions due to low mixing layers heights and vice versa. Significantly lower values for EBC and particle number concentration were registered during weekends (Figure 3b), when also traffic volume showed a reduction of about 25% compared to working days (traffic data from ARPA Lombardia), further showing the role of the traffic source above mentioned.

The impact of wood burning was assessed through source apportionment as described in detail in the next section.

3.2 PM1 source apportionment

As already mentioned in section 2.2, Positive Matrix Factorization model was applied to PM1 data collected during winter 2012. The dataset comprised 17 variables (mass, Si, K, Ca, Ti, Mn, Fe, Cu, Zn, Br, Pb, OC, EC, NO_3^-, SO_4^{2-}, NH_4^+, levoglucosan) and 109 data entries.

Factor labelling was accomplished according to percentage of species and the chemical profile (represented as dots and bars, respectively, in Figure 4 a-g). Percentages higher than 0.3 were considered as significant and the factor-to-source assignments were nitrate, sulphate, wood burning, industry, traffic, fine dust and a Pb-rich source. Average nighttime and daytime source apportionments are reported in Figure 5 and Table S2 (Supplementary Material).

Except for wood burning, which was consistently higher (on average +7%) during the night, source contributions did not show significant differences between daytime and nighttime, although on daytime all other resolved factors (but Pb-rich) showed slightly higher percentages (differences in the range 0.7 - 1.9%, see Table S2, Supplementary Material).

306 It is worth noting that in all chemical profiles there was OC, which was likely a signal for the
307 presence of highly oxygenated compounds in the sub-micron PM fraction due to aerosol aging
308 related to relatively long atmospheric residence times already mentioned.
309 Factor 1 was interpreted as "Nitrate" as NO_3^- and NH_4^+ showed both high percentages (i.e. 98% of
310 nitrate and 74% of ammonium were found in this factor) and significant concentrations in the
311 chemical profile. The nitrate-to-ammonium ratio was 3.4 suggesting that ammonium nitrate was the
312 most likely nitrate compound as the computed ratio was stoichiometrically consistent. It was the
313 most relevant contributor accounting on average for 37% of PM1 mass.
314 SO_4^{2-} was found only in Factor 2 thus strongly bounding the assignment to this compound and the
315 factor was labelled as "Sulphate". It explained on average 19% of PM1 mass.
316 In Factor 3 the tracer element according to its relative contribution was levoglucosan but also K
317 gave a not negligible contribution (34%). It was named "Wood burning" as levoglucosan and
318 potassium (especially soluble K) in PM fine fraction are often considered as good markers for wood
319 burning especially during wintertime when levoglucosan degradation is generally considered
320 negligible. Our previous work (Bernardoni et al., 2011) at the same location already pointed to
321 wood burning as a not negligible contributor (14%) to wintertime PM10 mass. In fact, in the urban
322 area of Milan the use of wood/pellet-fed stoves for residential heating is increasing likely because
323 of economic incentives for using renewable energy sources and the higher price of methane as a
324 fuel (Pastorello et al., 2011). In this study, wood burning on average accounted for 13% of PM1
325 mass and it is noteworthy that this was the only factor showing a significant difference between
326 night and day. Average nighttime (i.e. 19-04 time interval) contributions were as high as 16% while
327 during daytime this source explained 9% of the PM1 mass.
328 In Factor 4, percentages higher than 50% were found for Fe, Cu, and EC thus it was associated to
329 the traffic source as these aerosol components are tracers of traffic (Pant and Harrison, 2013; Viana
330 et al., 2008). The chemical profile, as expected, was especially enriched in OC and EC. In PM1 the
331 average (primary) traffic contribution was estimated to be 12%.
332 Factor 5 was characterised by Mn and Zn as tracer elements (i.e. percentage contribution higher
333 than 65%) and it was associated to industrial emissions, according to previous results found by our
334 group at the same sampling site for PM10, PM2.5 and PM1 (Marcazzan et al., 2001; Vecchi et al.,
335 2008a) as well as by other authors (e.g. Dall'Osto et al., 2013; and references therein). The
336 contribution of this source to PM1 mass was 9%.
337 Factor 6 showed percentages higher than 70% for Si, Ca, and Ti suggesting the impact from fine
338 dust. The levoglucosan presence in the chemical profile was anomalous but looking at the statistics
339 of bootstrap in this factor the variability (i.e. the ratio between standard deviation and mean values)

for this factor was pretty high (i.e. larger than 70%) thus indicating that this species was not very much relevant in this factor. This factor accounted for 4.3% of the PM1 mass.

In factor 7 lead was the tracer element (100% of species contribution) therefore the source – contributing on average for 5% to PM1 mass - was labelled as Pb-rich although in the chemical profile carbonaceous components, nitrate, potassium and zinc gave a not negligible contribution. This source needs further investigation although literature works point at a variety of sources for Pb such as coal combustion, waste incinerators or metallurgical processes (e.g. Widory et al., 2004; Zhang et al., 2009). In Milan coal combustion is not expected to be a relevant contributor as residential heating is dominated by natural gas fuel and biomass combustion; moreover, only one 70MW plant for energy production using coal is still operating in the region at a site which is more than 90 km far away. Four waste incinerators as well as some metallurgical industries are present in the Milan surroundings and could be likely associated to this factor. A more detailed PM1 characterisation – possibly using high-time resolution data – might better elucidate the specific source associated to the Pb-rich factor singled out in this source apportionment study.

3.3 Chemical extinction coefficient of PM1 and source apportionment of light extinction

On average (Table 2), among the aerosol components the major contributor to total light extinction coefficient (b_{ext}) was ammonium nitrate (34.1%), followed by organic matter (27.0%), light absorption components (b_{ap}) consisting primarily of black carbon (10.5%), ammonium sulphate (8.5%), and coarse mass (7.3%). As expected, in PM1 fine soil was almost a negligible contributor (0.4%) to b_{ext}. The Rayleigh scattering term - due to atmospheric gases and NO_2 absorption - overall explained 12.1% of b_{ext}. From light extinction coefficient b_{ext} the visual range (VR, in km see Table 2) was also estimated using the Koschmieder equation VR = (3.912/bext) x 1000.

To the authors' knowledge, the literature data on chemical/reconstructed extinction at urban sites refer mainly to Chinese towns (examples are Xi'an, Taichung, Xiamen, Hong Kong, Guangzhou, Baoji, Beijing, Hangzhou, and Shanghai). On average, b_{ext} in Milan was much lower (i.e. about a factor 3-5) than values reported in Chinese cities (see for example Cao et al. 2012; Wang et al. 2015a,b); on the contrary, comparable b_{ext} wintertime values were found at a Chinese suburban site (Deng et al., 2016). OM – which was one component accounting for a significant part of the light extinction in Milan - was reported as the largest contributor to b_{ext} by some authors (e.g. Wang et al., 2015a and 2016; Xiao et al., 2014) and in those papers ammonium nitrate typically accounted for approximately 20% of b_{ext}. Cao et al. (2012) reported that OM was the second largest contributor when considering data corresponding to a visual range higher than 10 km; this is comparable to what detected for Milan in this work where a VR higher than 10 km was recorded in

approximately in 80% of the days and where OM represents the second largest contributor to light extinction. Cao et al. (2012) in all other cases – corresponding to much lower visual range values – reported that the dominant component was ammonium sulphate, in agreement with what found at other Chinese cities and at non-urban IMPROVE sites (Malm and Day, 2000) where percentages of about 40% and 60%, respectively, were recorded. It is noteworthy that this was never the case in our study where on average this component accounted for less than 9%. Temporal patterns of $b_{ext,aer}$ (Figure S4, Supplementary Material) showed that the contribution due to organic matter and ammonium nitrate was often comparable but when the highest $b_{ext,aer}$ occurred ammonium nitrate generally contributed at most. Ammonium nitrate during wintertime in Milan was by far the most important component causing visibility impairment and accounting for 42% of $b_{ext,aer}$. In Milan, the relationship between VR and light extinction due to ammonium nitrate and OM could be well represented by a decreasing power law with R^2 higher than 0.85 while it decreased to 0.5 for ammonium sulphate (not shown).

The source apportionment of aerosol light extinction is reported in Table 3. Results show that considering all samples together, nitrate contributed at most (on average 41.6%) with no significant daytime-nighttime difference and $b_{ext,aer}$ was accounted for by sulphate, traffic, and wood burning as much as 18.3%, 17.8%, and 12.4%, respectively. In Milan secondary inorganic aerosols (i.e. sulphate and nitrate) gave a very high contribution (up to 60%) to $b_{ext,aer}$ which was typically much higher than most of the results reported in literature works for Chinese towns (i.e. Gao et al., 2015; Wang et al., 2016 ; Xiao et al., 2014). Opposite, traffic contribution to $b_{ext,aer}$ in Milan is low compared to some literature estimates for Chinese sites (e.g. Gao et al., 2015; Wang et al., 2016) giving two-fold higher values. Nevertheless, it is important to note that in literature works a large variability exists on the contribution to light extinction due to traffic, ranging from less than 10% up to 40%. Another not negligible contribution was given by wood burning, which resulted comparable to estimates reported in literature works ranging from 4 to 25% (e.g. Chen et al., 2014; Xiao et al., 2014).

Conclusions

Light extinction and visibility are environmental challenges at many polluted areas where emissions from different sources impact on air quality. Visibility impairment not only affects the aesthetic perception of population but it is strictly related to air quality degradation. The IMPROVE algorithm is a well-known and simple method to estimate chemical light extinction using PM data available at monitoring networks. In this work, the assessment of the chemical light extinction (b_{ext}) due to different PM1 components and sources was achieved applying a tailored approach based on

site-specific extinction coefficients and using f(RH) coefficients for all the relevant aerosol components aiming at reducing uncertainties and assumptions typically affecting the IMPROVE algorithm.

Data on PM1 composition and sources are still scarce in the literature especially evaluating daytime and nighttime contributions, separately; moreover, as far as we know, this is the first time that the assessment of aerosol light extinction retrieved from aerosol chemical components data is reported for a hot-spot pollution site in Europe. PM1 chemical characterisation highlighted the important role played by secondary aerosols, which contributed as much as 63% to PM1 mass; this result is particularly relevant in a pollution hot spot area where reduction strategies do not produce the attainment of air quality standards for PM yet. In this work, total light extinction coefficient on average was 287 Mm^{-1} corresponding to approximately 19 km as visual range. Major contributions from aerosol components as well as aerosol sources were estimated pointing at the role of secondary components, followed by traffic and wood burning.

Acknowledgements

This work was partly funded by the National Institute of Nuclear Physics under INFN-experiments MANIA and DEPOTMASS.

The authors acknowledge ARPA Lombardia for availability of gaseous pollutants and traffic data, dr. Alessandro Bigi for having provided SMPS data, dr. Miriam Elser for size-segregated aerosol distributions measurements, and dr. Federica Crova for estimates of aerosol residence times.

References

Bernardoni,V., Vecchi, R., Valli, G., Piazzalunga, A., and Fermo, P., (2011). PM10 source apportionment in Milan (Italy) using time-resolved data. Science of the Total Environment, 409, 4788-4795.

Bernardoni, V., Elser, M., Valli, G., Valentini, S., Bigi, A., Fermo, P., Piazzalunga, A., and Vecchi, R. (2017). Size-segregated aerosol in a hot-spot pollution urban area: Chemical composition and three-way source apportionment. Environmental Pollution 231, 601-611.

Bigi, A., and Ghermandi, G., (2011). Particle Number Size Distribution and Weight Concentration of Background Urban Aerosol in a Po Valley Site. Water, Air, and Soil Pollution, 220(1), 265-278.

Cao, J., Wang, Q., Chow, J.C., Watson, J.G., Tie, X., Shen, Z., Wang, P., and An, Z., (2012). Impacts of aerosol compositions on visibility impairment in Xi'an, China. Atmospheric Environment, 59, 559-566.

441 Carozzi, M., Ferrara, R.M., Fumagalli, M., Sanna, M., Chiodini, M., Perego, A., Chierichetti, A.,
442 Brenna, S., Rana, G., and Acutis, M., (2012). Field-scale ammonia emissions from surface
443 spreading of dairy slurry in Po Valley. Italian Journal of Agrometeorology, 3, 25-34.
444 Chen, W.-N-, Chen, Y.-C., Kuo, C.-Y., Chou, C.-H., Cheng, C.-H., Huang, C.-C., Chang, S.-Y.,
445 Raman, M.R., Shang, W.-L., Chuang, T.-Y., and Liu, S.-C., (2014). The real-time method of
446 assessing the contribution of individual sources on visibility degradation in Taichung. Science of
447 the Total Environment, 497-498, 219-228.
448 Corsini, E., Vecchi, R., Marabini, L., Fermo, P., Becagli, S., Bernardoni, V., Caruso, D., Corbella,
449 L., Dell'Acqua, M., Galli, C.L., Lonati, G., Ozgen, S., Papale, A., Signorini, S., Tardivo, R., Valli,
450 G., and Marinovich, M., (2017). The chemical composition of ultrafine particles and associated
451 effects at an alpine town impacted by wood burning. Science of the Total Environment, 587-588,
452 223-231.
453 Crova, F., (2017). Studio dei tempi di residenza degli aerosol atmosferici mediante la misura del
454 disequilibrio di radionuclidi naturali. Degree Thesis in Physics, University of Milan (in Italian).
455 Dall'Osto, M., Querol, X., Amato, F., Karanasiou, A., Lucarelli, F., Nava, S., Calzolai, G., and
456 Chiari, M., (2013). Hourly elemental concentrations in PM2.5 aerosols sampled simultaneously at
457 urban background and road site during SAPUSS – diurnal variations and PMF receptor modeling.
458 Atmospheric Chemistry and Physics, 13, 4375-4392.
459 Deng, J., Zhang, Y., Hong, Y., Xu, L., Chen, Y., Du, W., and Chen, J., (2016). Optical properties of
460 PM2.5 and the impacts of chemical compositions in the coastal city Xiamen in China. Science of
461 the Total Environment, 557-558, 665-675.
462 Eatough, D.J., and Farber, R., (2009). Apportioning visibility degradation to sources of PM2.5
463 using Positive Matrix Factorization. Journal of the Air and Waste Management Association, 59,
464 1092-1110.
465 Elser Fritsche, M., (2012). Le particelle ultrafini in atmosfera: metodi di campionamento e
466 caratterizzazione. Master degree thesis in Physics, Università degli Studi di Milano (in Italian).
467 EAA, European Environmental Agency, (2011). IP/11/645 Press release.
468 EAA, European Environmental Agency, (2016). Air quality in Europe — 2016 report. No 28/2016.
469 Gao, Y., Lai, S., Lee, S.-C., Yau, P.S., Cheng, Y., Wang, T., Xu, Z., Yuan, C., and Zhang, Y.,
470 (2015). Optical properties of size.resolved particles at Hong Kong urban site during winter.
471 Atmospheric Research, 155, 1-12.
472 Giugliano, M., Lonati, G., Butelli, P., Romele, L., Tardivo, R., and Grosso, M., (2005). Fine
473 particulate (PM2.5–PM1) at urban sites with different traffic exposure. Atmospheric Environment,
474 39, 2421-2431.

475 Heinzerling, A., Hsu, J., and Yip, F., (2016). Respiratory health effects of ultrafine particles in
476 children: a literature review. Water, Air and Soil Pollution, 227, 32.
477 Hyvärinen, A.-P., Vakkari, V., Laakso, L., Hooda, R.K, Sharma, V. P., Panwar, T.S., Beukes, J.P.,
478 van Zyl, P., Josipovic, M., Garland, R.M., Andreae, M.O., Pöschl, U., and Petzold, A., (2013).
479 Correction for a measurement artifact of the Multi-Angle Absorption Photometer (MAAP) at high
480 black carbon mass concentration levels. Atmospheric Measurement Techniques, 6, 81-90.
481 Invernizzi, G., Ruprecht, A., Mazza, R., De Marco, C., Mocnik, G., Sioutas, C., and Westerdahl, D.,
482 (2011). Measurement of black carbon concentration as an indicator of air quality benefits of traffic
483 restriction policies within the ecopass zone in Milan, Italy. Atmospheric Environment, 45, 3522-
484 3527.
485 Jaffrezo, J.-L., Aymoz, G., Delaval, C., and Cozic, J., (2005). Seasonal variations of the water
486 soluble organic carbon mass fraction of aerosol in two valleys of the French Alps. Atmospheric
487 Chemistry and Physics, 5, 2809–2821.
488 Li, W., Sun, J., Xu, L., Shi, Z., Riemer, N., Sun, Y., Fu, P., Zhang, J., Lin, Y., Wang, X., Shao, L.,
489 Chen J., Zhang, X., Wang, Z., and Wang, W. (2016). A conceptual framework for mixing structures
490 in individual aerosol particles. Journal of Geophysical Research: Atmospheres, 121 (22), 13784–
491 13798.
492 Malm, W.C., Sisler, J.F., Huffman, D., Eldred, R.A., and Cahill, T.A., (1994). Spatial and seasonal
493 trends in particle concentration and optical extinction in the United States. Journal of Geophysical
494 Research, 99, 1347-1370.
495 Malm, W.C., and Day, D.E., (2000). Optical properties of aerosols at Gran Canyon national park.
496 Atmospheric Environment, 34, 3373-3391.
497 Marcazzan, G.M., Vaccaro, S., Valli, G., and Vecchi, R., (2001). Characterisation of PM10 and
498 PM2.5 particulate matter in the ambient air of Milan (Italy). Atmospheric Environment, 35, 4639-
499 4650.
500 Marcazzan, G.M., Caprioli, E., Valli, G., and Vecchi, R., (2003). Temporal variation of ^{212}Pb
501 concentration in outdoor air of Milan and a comparison with ^{214}Bi. Journal of Environmental
502 Radioactivity, 65, 77-90.
503 Mazzei, F., Lucarelli, F., Nava, S., Prati, P., Valli, G., and Vecchi, R., (2007). A new
504 methodological approach: the combined use of two-stage streaker samplers and optical particle
505 counters for the characterization of airborne particulate matter. Atmospheric Environment, 41,
506 5525-5535.
507 Norris, G., Duvall, R., Brown, S., and Bai, S., (2014). EPA Positive Matrix Factorization (PMF)
508 5.0. Fundamentals and user guide. EPA/600/R-14/108 U.S. Environmental Protection Agency

509 Paatero, P., (2000). User's Guide for the Multilinear Engine Program “ME2” for Fitting Multilinear
510 and Quasi-multilinear Models.
511 Paatero, P., (2015). User’s Guide for Positive Matrix Factorization Programs PMF2 and PMF3, Part
512 1: Tutorial. University of Helsinki: Helsinki, Finland (last changed on 31 March 2015)
513 Pant, P., and Harrison, R.M., (2013). Estimation of the contribution of road traffic emissions to
514 particulate matter concentrations from field measurements: A review. Atmospheric Environment,
515 77, 78-97.
516 Pastorello, C., Caserini, S., Galante, S., Dilara, P., and Galletti, F., (2011). Importance of activity
517 data for improving the residential wood combustion emission inventory at regional level.
518 Atmospheric Environment, 45, 2869-2876.
519 Pérez, N., Pey, J., Querol, X., Alastuey, A., Lopez, J.M., and Viana, M., (2008). Partitioning of
520 major and trace components in PM10-PM2.5-PM1 at an urban site in Southern Europe.
521 Atmospheric Environment, 42, 1677-1691.
522 Perrone, M.R., Becagli, S., Orza, J.A.G., Vecchi, R., Dinoi, A., Udisti, R., and Cabello, M., (2013).
523 The impact of long-range-transport on PM1 and PM2.5 at a Central Mediterranean site.
524 Atmospheric Environment, 71, 176-186.
525 Petzold, A., Ogren, J.A., Flebig, M., Laj, P., Li, S.-M., Baltensperger, U., Holzer-Popp, T., Kinne,
526 S., Pappalardo, G., Sugimoto, N., Wehrli, C., Wiedensohler, A., and Zhang, X.-Y., (2013).
527 Recommendations for reporting “black carbon” measurements. Atmospheric Chemistry and
528 Physics, 13, 8365–8379.
529 Piazzalunga, A., Fermo, P., Bernardoni, V., Vecchi, R., Valli, G., and De Gregorio, M.A., (2010). A
530 simplified method for levoglucosan quantification in wintertime atmospheric particulate matter by
531 High Performance Anion-Exchange Chromatography coupled with Pulsed Amperometric
532 Detection. International Journal of Environmental Analytical Chemistry, 90(12), 934-947.
533 Piazzalunga, A., Bernardoni, V., Fermo, P., and Vecchi, R., (2013). Optimisation of analytical
534 procedures for the quantification of ionic and carbonaceous fractions in the atmospheric aerosol and
535 application to ambient samples. Analytical Bioanalytical Chemistry, 405, 1123-1132.
536 Pitchford, M., Malm, W., Schichtel, B., Kumar, N., Lowenthal, D., and Hand, J., (2007). Revised
537 algorithm for estimating light extinction from IMPROVE particle speciation network. Journal of
538 Air and Waste Management Association, 57, 1236-1336.
539 Polissar, A.V., Hopke, P.K., Paatero, P., Malm, W.C., and Sisler, J.F., (1998). Atmospheric aerosol
540 over Alaska - 2. Elemental composition and sources. Journal of Geophysical Research, 103, 19045-
541 19057.

542 Poluzzi, V., Bacco, D., Bonafé, G., Maccone, C., Ferrari, S., Vecchi, R., Decesari, S., and
543 Ricciardelli, I., (2013). Meteorological and chemical factors triggering an exceptional PM pollution
544 episode in wintertime in the Po valley, Italy. Poster presentation C174, European Aerosol
545 Conference EAC2013, Prague, Sept. 1-6 2013.
546 Putaud, J.P., Van Dingenen, R., and Raes, F., (2002). Submicron aerosol mass balance at urban and
547 semirural sites in the Milan area (Italy). Journal of Geophysical Research, 107 D22, 8198-8208.
548 Reche, C., Querol, X., Alastuey, A., Viana, M., Pey, J., Moreno, T., Rodriguez, S., Gonzalez, Y.,
549 Fernandez-Camacho, R., Sanchez de la Campa, A.M., de la Rosa, J., Dall'Osto, M., Prevot, A.S.H.,
550 Hueglin, C., Harrison, R.M., and Quincey, P., (2011). New considerations for PM, Black Carbon
551 and particle number concentration for air quality monitoring across different European cities.
552 Atmospheric Chemistry and Physics, 11, 6207-6227.
553 Rogula-Kozłowska, W., and Keljnowski, K., (2013). Submicrometer aerosol in rural and urban
554 backgrounds in Southern Poland: Primary and secondary components of PM1. Bulletin of
555 Environmental Contamination and Toxicology, 90, 103-109.
556 Tao, J., Zhang, L., Ho, K., Zhang, R., Lin, Z., Zhang, Z., Lin, M., Cao, J., Liu, S., and Wang, G.,
557 (2014). Impact of PM2.5 chemical compositions on aerosol light scattering in Guangzhou — the
558 largest megacity in South China. Atmospheric Research, 135–136, 48–58.
559 Theodosi, C, Grivas, G., Zarmpas, P., Chaloulakou, A., and Mihalopoulos, N., (2011). Mass and
560 chemical composition of size-segregated aerosols (PM1, PM2.5, PM10) over Athens, Greece: local
561 versus regional sources. Atmospheric Chemistry and Physics, 11, 11895-11911.
562 Turpin, B.J., and Huntzicker, J.J., (1995). Identification of secondary organic aerosol episodes and
563 quantitation of primary and secondary organic aerosol concentrations during SCAQS. Atmospheric
564 Environment, 29(23), 3527-3544.
565 Valentini, S., (2016). Determinazione del coefficiente di estinzione a più lunghezze d'onda in
566 campioni di aerosol atmosferico mediante approcci sperimentali e modellistici. Master degree thesis
567 in Physics, Università degli Studi di Milano (in Italian).
568 Valentini, S., Bernardoni, V., Massabò, D., Prati, P., Valli, G., and Vecchi, R. Tailoring coefficients
569 in the IMPROVE algorithm to assess site-specific reconstructed light extinction. Accepted for
570 publication in Atmospheric Environment.
571 Van Damme, M, Wichink Kruit, R.J., Schaap, M., Clarisse, L., Clerbaux, C., Coheur, P.-F.,
572 Dammers, E., Dolman, A.J., and Erisman, J.W., (2016). Evaluating 4 years of atmospheric
573 ammonia (NH3) over Europe using IASI satellite observations and LOTOS-EUROS model results.
574 Journal of Geophysical Research: Atmospheres, 119, 9549–9566.

575 Vecchi, R., Marcazzan, G., Valli, G., Ceriani, M., and Antoniazzi, C., (2004). The role of
576 atmospheric dispersion in the seasonal variation of PM1 and PM2.5 concentration and composition
577 in the urban area of Milan (Italy). Atmospheric Environment, 38, 4437-4446.
578 Vecchi, R., Marcazzan, G., and Valli, G., (2005). Seasonal variation of ^{210}Pb activity concentration
579 in outdoor air of Milan (Italy). Journal of Environmental Radioactivity 82, 251-266.
580 Vecchi, R., Chiari, M., D'Alessandro, A., Fermo, P., Lucarelli, F., Mazzei, F., Nava, S.,
581 Piazzalunga, A., Prati, P., Silvani, F., and Valli, G., (2008a). A mass closure and PMF source
582 apportionment study on the sub-micron sized aerosol fraction at urban sites in Italy. Atmospheric
583 Environment, 42, 2240-2253.
584 Vecchi, R., Bernardoni, V., Fermo, P., Piazzalunga, A., and Valli, G., (2008b). Il PM10 a Milano:
585 risultati di una campagna di misura invernale. Poster presentation PA5-068 at the 3° National
586 Congress on Particulate Matter, PM2008, Bari (Italy), October 6-8 (in Italian).
587 Vecchi, R., Bernardoni, V., Fermo, P., Lucarelli, F., Mazzei, F., Nava, S., Piazzalunga, A., Prati, P.,
588 and Valli, G., (2009). 4-hours resolution data to study PM10 in a "hot spot" area in Europe.
589 Environmental Monitoring and Assessment, 154, 283-300.
590 Vecchi, R., Bernardoni, V., Paganelli, C., and Valli, G., (2014). A filter-based light-absorption
591 measurement with polar photometer: Effects of sampling artefacts from organic carbon. Journal of
592 Aerosol Science, 70, 15-25.
593 Viana, M., Kuhlbusch, T.A.J., Querol, X., Alastuey, A., Harrison, R.M., Hopke, P.K., Winiwarter,
594 W., Vallius, M., Szidat, S., Prévôt, A.S.H., Hueglin, C., Bloemen, H., Wåhlin, P., Vecchi, R.,
595 Miranda, A.I., Kasper-Giebl, A., Maenhaut, W., and Hitzenberger, R., (2008). Source
596 apportionment of PM in Europe: a review of methods and results. Journal of Aerosol Science, 39,
597 827-849.
598 Xiao, S., Wang, Q.Y., Cao, J.J., Huang, R.-J., Chen, W.D., Han, Y.M., Xu, H.M., Liu, S.X., Zhou,
599 Y.Q., Wang, P., Zhang, J.Q., and Zhan, C.L., (2014). Long-term trends in visibility and impacts of
600 aerosol composition on visibility impairment in Baoji, China. Atmospheric Research, 149, 88-95.
601 Wang, H., Tian, M., Li, X., Chang, Q., Cao, J., Yang, F., Ma, Y., and He, K., (2015a). Chemical
602 composition and light extinction contribution of PM2.5 in urban Beijing for a 1-year period.
603 Aerosol and Air Quality Research, 15, 2200-2211.
604 Wang, H., Li, X., Shi, G., Cao, J., Li, C., Yang, F., Ma, Y., and He, K., (2015b). PM2.5 chemical
605 compositions and aerosol optical properties in Beijing during the late fall. Atmosphere, 6, 164-182.
606 Wang, J., Zhang, Y.-f., Feng, Y.-c., Zheng, X.-j., Jiao, L., Hong, S.-m-, Shen, J.-d., Zhu, T., Ding,
607 J., and Zhang, Q., (2016). Characterization and source apportionment of aerosol light extinction

608 with a coupled model of CMB-IMPROVE in Hangzhou, Yangtze River Delta of China.
609 Atmospheric Research, 178-179, 570-579.
610 Watson, J.G., (2002). Visibility: Science and Regulation. Journal of Air and Waste Management
611 Association, 52, 628-713.
612 Widory, D., Roy, S., Le Moullec, Y., Goupil, G., Cocherie, A., and Guerrot, C., (2004). The origin
613 of atmospheric particles in Paris: a view through carbon and lead isotopes. Atmospheric
614 Environment, 38, 953-961.
615 Zhang, Y., Wang, X., Chen, H., Yang, X., Chen, J., and Allen, J.O., (2009). Source apportionment
616 of lead-containing aerosol particles in Shanghai using single particle mass spectrometry.
617 Chemosphere, 74, 501-507.

Figure captions

Figure 1: PM1 components concentration (in ng/m^3) in Milan during the winter campaign in 2012.

Figure 2: temporal patterns of Rn-222 (in Bq/m^3) and EBC (in μg/m^3) concentrations during the monitoring campaign.

Figure 3 (a-b): mean daily patterns for **a)** particle number concentration (here particles with d<700 nm, in pp/cm^3), Equivalent Black Carbon concentration (EBC, in μg/m^3), NO_x concentration (in ppb/10), and Rn-222 concentration (in Bq/m^3); **b)** number particle concentration (in pp/cm^3) and EBC (in μg/m^3) given separately for working days (open symbols) and weekends (full symbols).

Figure 4 (a-g): Factors chemical profile and percentage of species in each factor for the 7-factor solution obtained by EPA-PMF with Fpeak=+0.5. Note that Nitr stands for Nitrate, Sulph for Sulphate, Amm for Ammonium, and Levo for Levoglucosan.

Figure 5: Source apportionment (in %) given for daytime and nighttime, separately.

Table 1: statistics on mass concentration (in µg/m^3) and relative contributions (in %) of PM1 components given for the whole dataset and for daytime (07-16 LT) and nighttime (19-04 LT) separately.

				All samples				
	Mass concentration (µg/m^3)	**Fine soil**	**Metal oxides**	**OM (OC·1.6)**	**EC**	**Nitrate**	**Sulphate**	**Ammonium**
mean	37.1	0.9%	1.7%	31.7%	7.9%	28.4%	6.3%	11.6%
median	33.0	0.7%	1.6%	30.5%	7.1%	28.2%	5.1%	11.5%
10°perc	15.9	0.3%	1.3%	24.0%	3.7%	15.2%	2.6%	7.1%
90°perc	63.5	1.7%	2.4%	40.9%	13.4%	43.4%	11.4%	15.8%

				Daytime samples (07-16 LT)				
	Mass concentration (µg/m^3)	**Fine soil**	**Metal oxides**	**OM (OC·1.6)**	**EC**	**Nitrate**	**Sulphate**	**Ammonium**
mean	36.5	1.0%	1.7%	30.2%	7.7%	28.7%	6.5%	12.1%
median	31.0	0.8%	1.5%	29.5%	6.7%	28.1%	5.3%	11.3%
10°perc	15.8	0.4%	1.2%	22.7%	3.7%	17.0%	2.6%	7.6%
90°perc	63.3	1.6%	2.3%	37.9%	12.4%	42.8%	11.5%	16.3%

				Nighttime samples (19-04 LT)				
	Mass concentration (µg/m^3)	**Fine soil**	**Metal oxides**	**OM (OC·1.6)**	**EC**	**Nitrate**	**Sulphate**	**Ammonium**
mean	37.8	0.8%	1.8%	33.3%	8.2%	28.1%	6.1%	11.1%
median	33.0	0.6%	1.7%	32.4%	7.2%	28.2%	4.7%	11.6%
10°perc	17.0	0.3%	1.3%	25.0%	3.7%	13.8%	2.5%	6.8%
90°perc	63.6	1.7%	2.6%	44.5%	13.7%	43.4%	11.0%	15.4%

Table 2: Statistics of light extinction coefficients b_{ext} (in Mm^{-1}) and visual range (VR, in km). Total number of samples: 110.

b_{ext} (in Mm^{-1})	Total	Amm. Sulphate	Amm. Nitrate	OM	b_{ap}	Fine Soil	Coarse Mass	Rayleigh Scattering	NO_2	VR (km)
mean	**287.2**	24.1	108.9	77.1	28.2	0.8	21.1	12.0	14.9	18.8
std. dev.	**158.1**	20.0	88.1	44.9	15.2	0.5	11.6	0.2	4.4	13.2
min	**45.0**	1.6	1.4	12.4	5.5	0.3	1.9	11.5	4.9	4.3
max	**919.9**	111.5	510.9	214.4	75.1	4.8	64.8	12.5	26.1	86.9
average percentage		**8.5%**	**34.1%**	**27.0%**	**10.5%**	**0.4%**	**7.3%**	**5.7%**	**6.4%**	

645
646 **Table 3:** Source apportionment of the extinction coefficient for atmospheric aerosols ($b_{ext, aer}$) in Mm^{-1} and %

647
648

	Sulphate	**Traffic**	**Pb-rich**	**Wood burning**	**Nitrate**	**Fine dust**	**Industry**	**$b_{ext,aer}$**
All data	38.5 Mm^{-1} **18.3%**	37.4 Mm^{-1} **17.8%**	15.3 Mm^{-1} **7.3%**	26.0 Mm^{-1} **12.4%**	87.5 Mm^{-1} **41.6%**	1.7 Mm^{-1} **0.8%**	6.0 Mm^{-1} **2.9%**	210.2 Mm^{-1}
Daytime data	39.0 Mm^{-1} **19.3%**	37.3 Mm^{-1} **18.4%**	14.6 Mm^{-1} **7.2%**	19.2 Mm^{-1} **9.5%**	85.7 Mm^{-1} **42.3%**	2.0 Mm^{-1} **1.0%**	6.3 Mm^{-1} **3.1%**	202.7 Mm^{-1}
Nighttime data	38.0 Mm^{-1} **17.5%**	37.5 Mm^{-1} **17.2%**	16.0 Mm^{-1} **7.3%**	32.3 Mm^{-1} **14.8%**	89.3 Mm^{-1} **41.1%**	1.5 Mm^{-1} **0.7%**	5.8 Mm^{-1} **2.7%**	217.5 Mm^{-1}

649
650

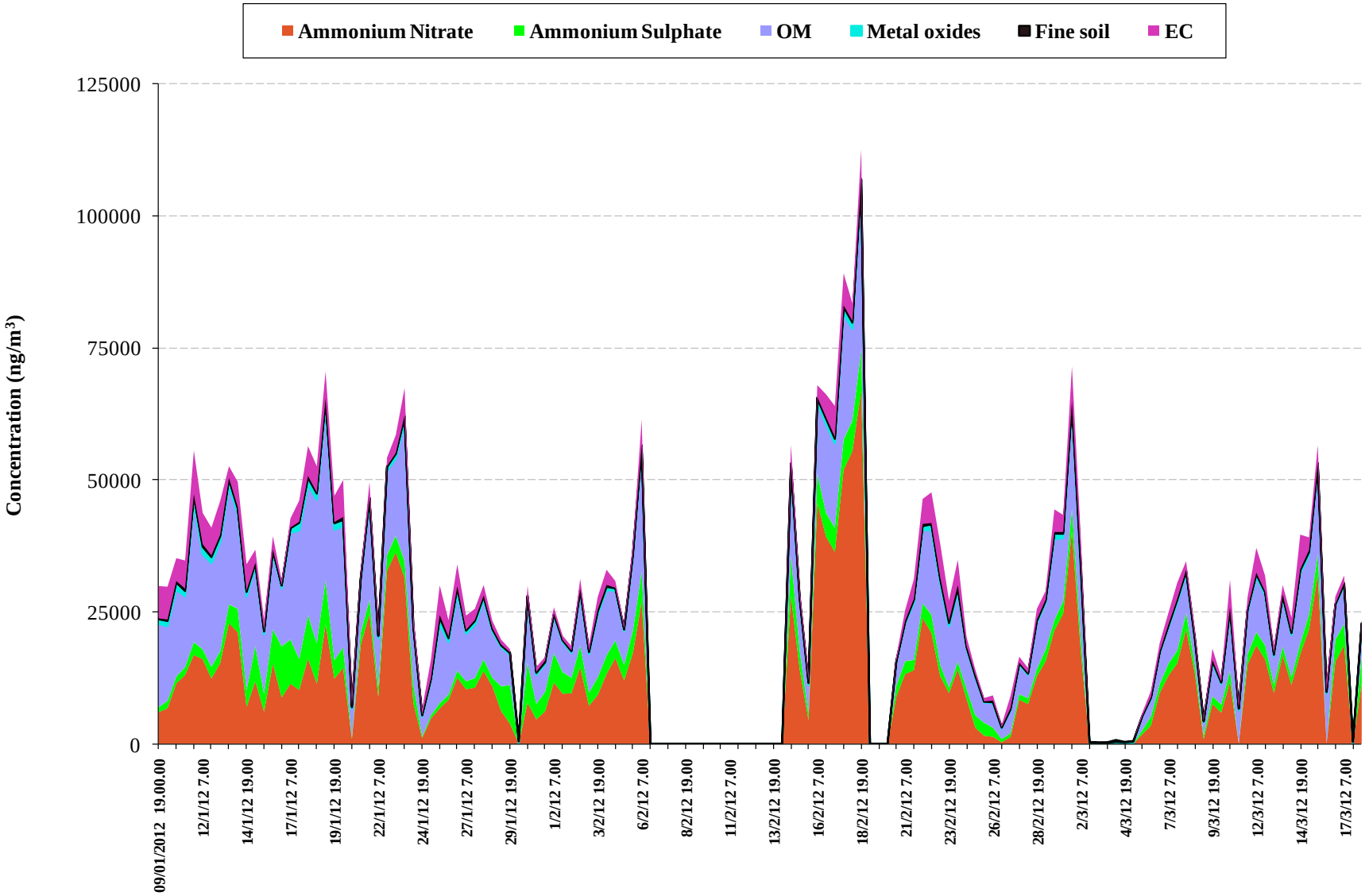
Ammonium Nitrate
Ammonium Sulphate
OM
Metal oxides
Fine soil
EC
Concentration (ng/m3)
125000
100000
75000
50000
25000
0
09/01/2012 19.00.00
12/1/12 7.00
14/1/12 19.00
17/1/12 7.00
19/1/12 19.00
22/1/12 7.00
24/1/12 19.00
27/1/12 7.00
29/1/12 19.00
1/2/12 7.00
3/2/12 19.00
6/2/12 7.00
8/2/12 19.00
11/2/12 7.00
13/2/12 19.00
16/2/12 7.00
18/2/12 19.00
21/2/12 7.00
23/2/12 19.00
26/2/12 7.00
28/2/12 19.00
2/3/12 7.00
4/3/12 19.00
7/3/12 7.00
9/3/12 19.00
12/3/12 7.00
14/3/12 19.00
17/3/12 7.00

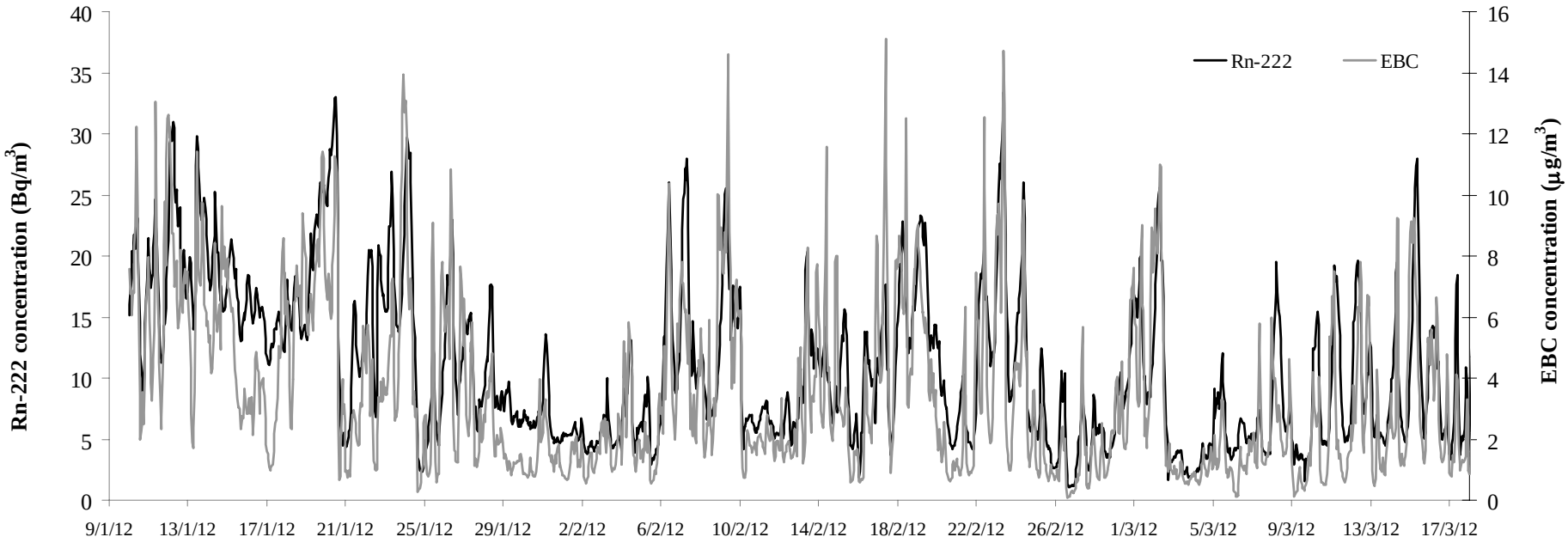
Rn-222
EBC
Rn-222 concentration (Bq/m3)
EBC concentration (µg/m3)
0
5
10
15
20
25
30
35
40
0
2
4
6
8
10
12
14
16
9/1/12
13/1/12
17/1/12
21/1/12
25/1/12
29/1/12
2/2/12
6/2/12
10/2/12
14/2/12
18/2/12
22/2/12
26/2/12
1/3/12
5/3/12
9/3/12
13/3/12
17/3/12

(a)

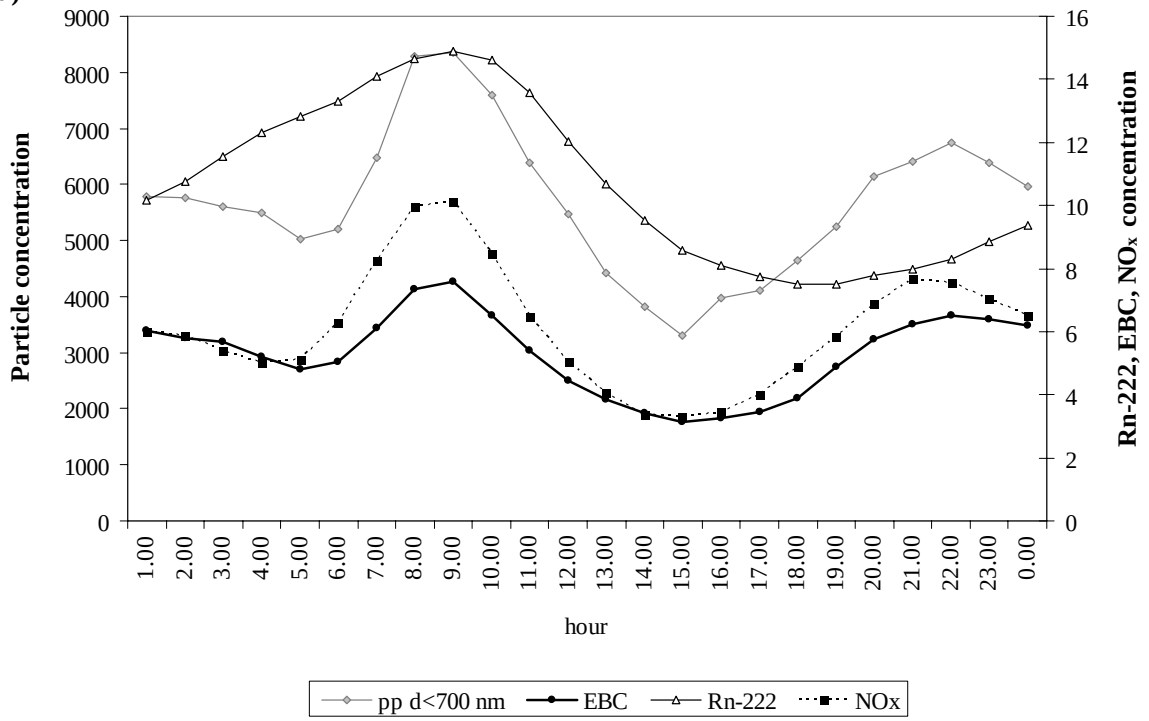
Particle concentration
Rn-222, EBC, NOx concentration
hour
pp d<700 nm
EBC
Rn-222
NOx

(b)

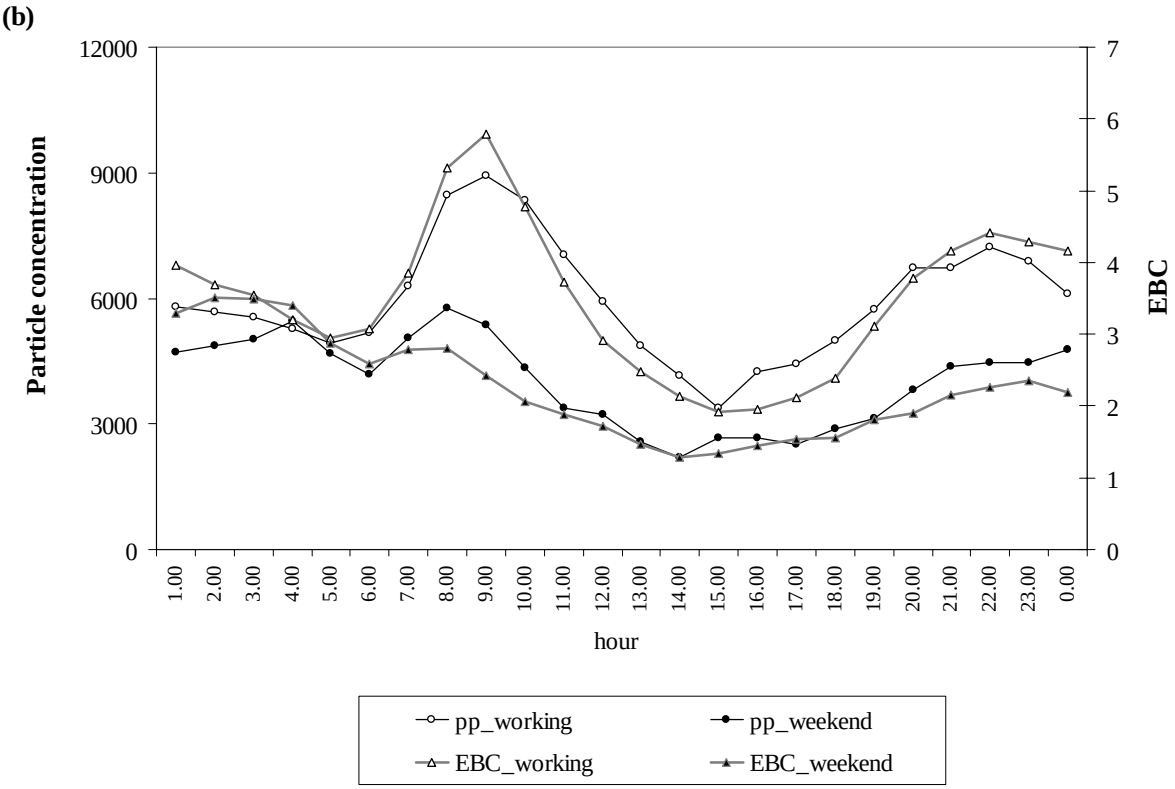
Particle concentration
EBC
hour
pp_working
pp_weekend
EBC_working
EBC_weekend

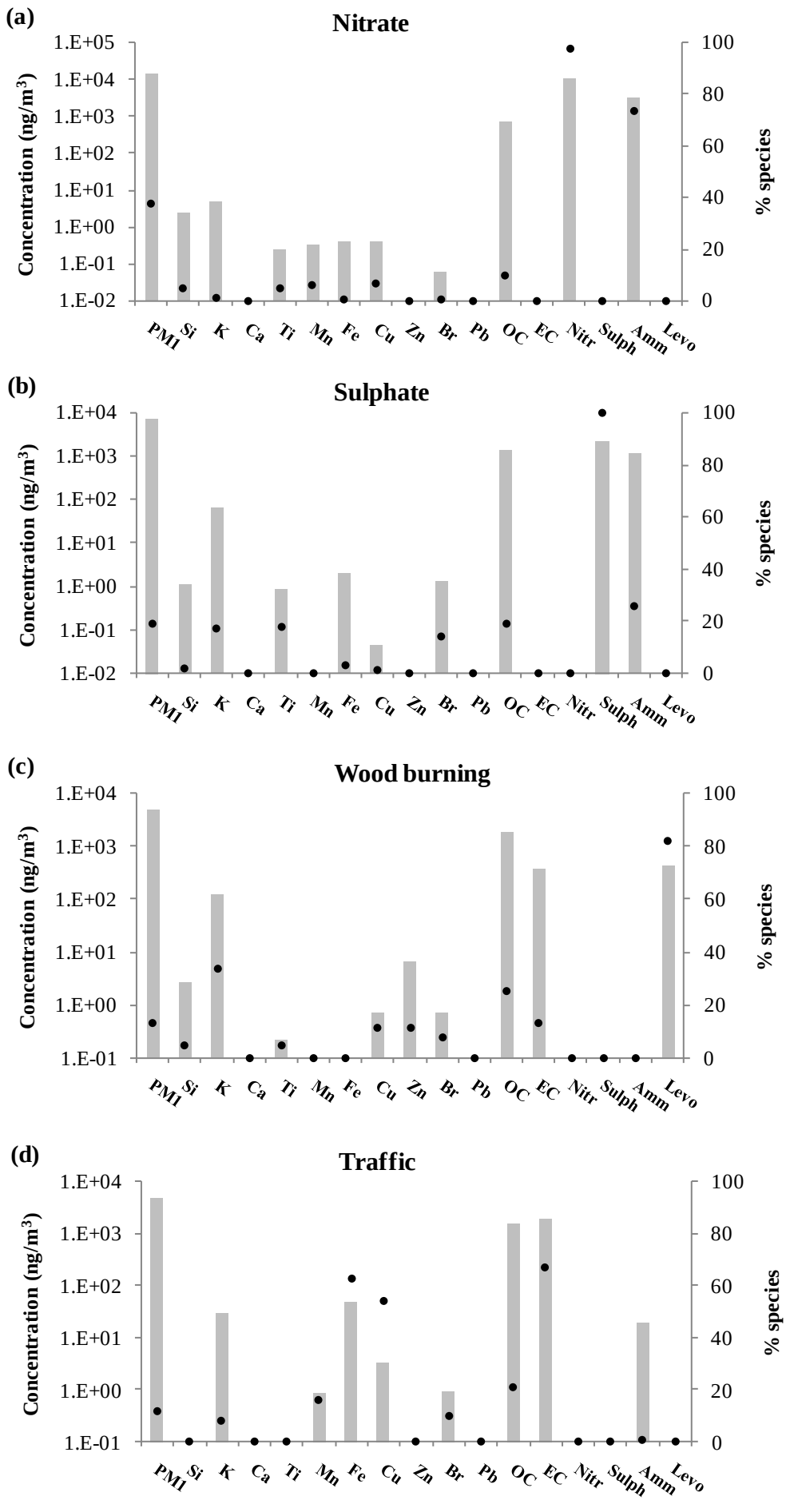
(a)
Nitrate
Concentration (ng/m3)
% species
1.E+05
1.E+04
1.E+03
1.E+02
1.E+01
1.E+00
1.E-01
1.E-02
100
80
60
40
20
0
PMI Si K Ca Ti Mn Fe Cu Zn Br Pb OC EC Nitr Sulph Amm Levo
(b)
Sulphate
Concentration (ng/m3)
% species
1.E+04
1.E+03
1.E+02
1.E+01
1.E+00
1.E-01
1.E-02
100
80
60
40
20
0
PMI Si K Ca Ti Mn Fe Cu Zn Br Pb OC EC Nitr Sulph Amm Levo
(c)
Wood burning
Concentration (ng/m3)
% species
1.E+04
1.E+03
1.E+02
1.E+01
1.E+00
1.E-01
100
80
60
40
20
0
PMI Si K Ca Ti Mn Fe Cu Zn Br Pb OC EC Nitr Sulph Amm Levo
(d)
Traffic
Concentration (ng/m3)
% species
1.E+04
1.E+03
1.E+02
1.E+01
1.E+00
1.E-01
100
80
60
40
20
0
PMI Si K Ca Ti Mn Fe Cu Zn Br Pb OC EC Nitr Sulph Amm Levo

(e)

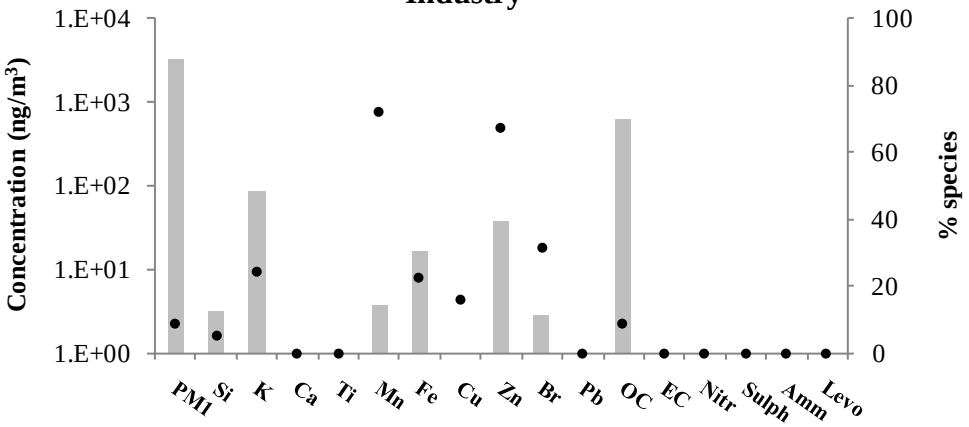
Industry
Concentration (ng/m3)
% species
1.E+04
1.E+03
1.E+02
1.E+01
1.E+00
100
80
60
40
20
0
PM1
Si
K
Ca
Ti
Mn
Fe
Cu
Zn
Br
Pb
OC
EC
Nitr
Sulph
Amm
Levo

(f)

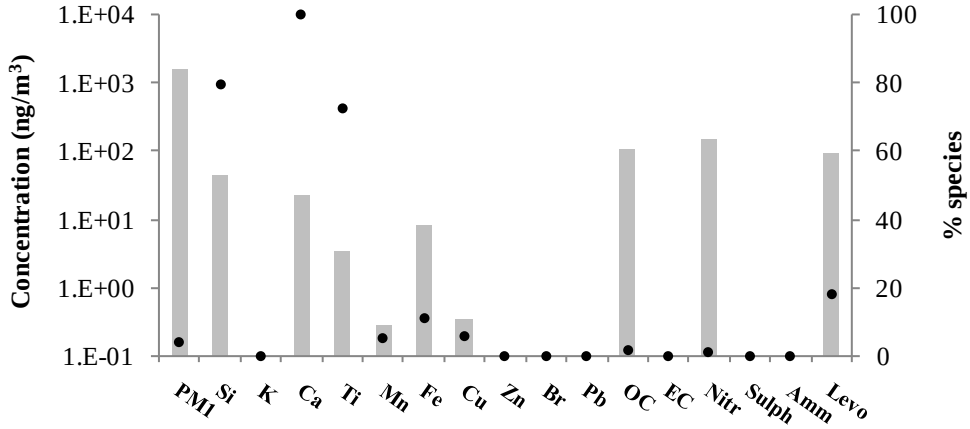
Fine dust
Concentration (ng/m3)
% species
1.E+04
1.E+03
1.E+02
1.E+01
1.E+00
1.E-01
100
80
60
40
20
0
PM1
Si
K
Ca
Ti
Mn
Fe
Cu
Zn
Br
Pb
OC
EC
Nitr
Sulph
Amm
Levo

(g)

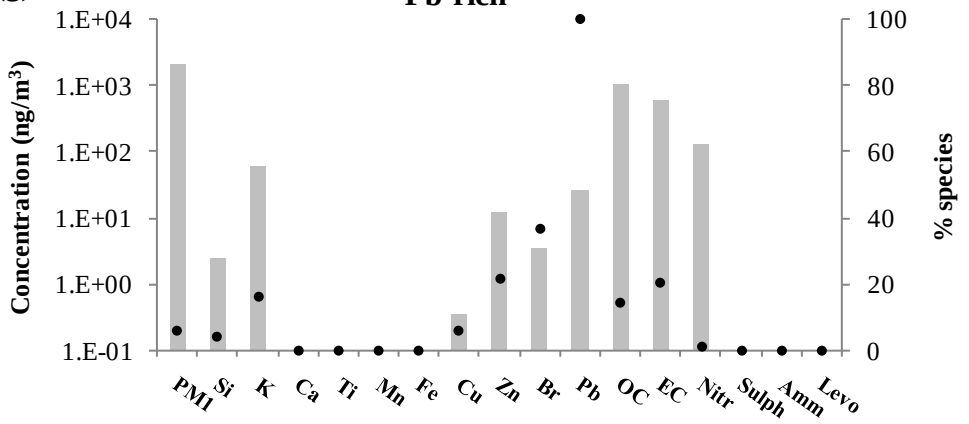
Pb-rich
Concentration (ng/m3)
% species
1.E+04
1.E+03
1.E+02
1.E+01
1.E+00
1.E-01
100
80
60
40
20
0
PM1
Si
K
Ca
Ti
Mn
Fe
Cu
Zn
Br
Pb
OC
EC
Nitr
Sulph
Amm
Levo

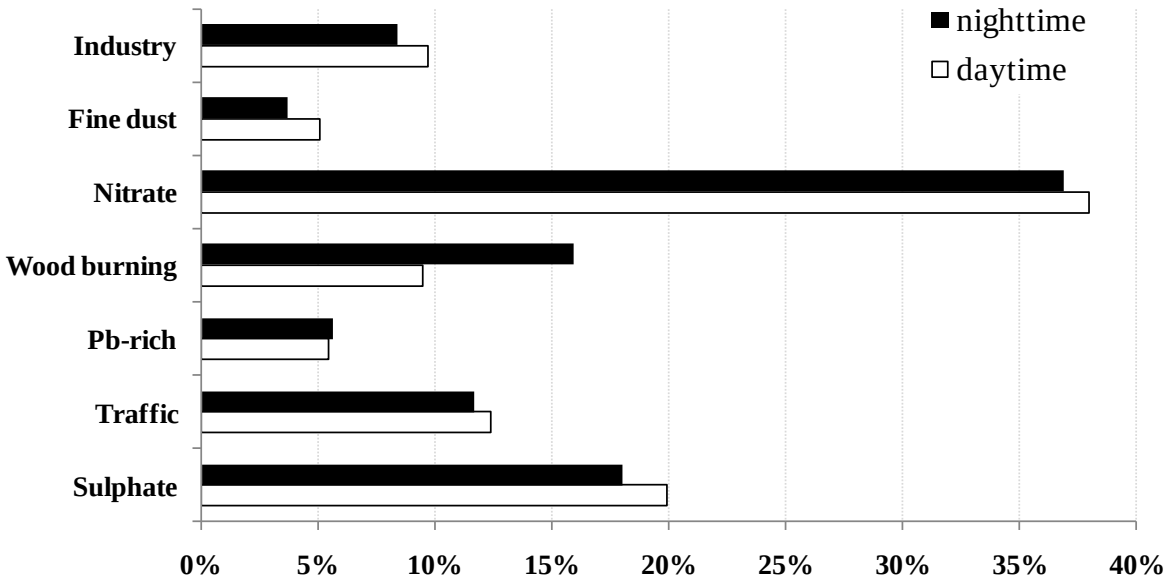
nighttime
daytime
Industry
Fine dust
Nitrate
Wood burning
Pb-rich
Traffic
Sulphate
0%
5%
10%
15%
20%
25%
30%
35%
40%

Supplementary Material

"Assessment of light extinction at a European polluted urban area during wintertime: Impact of PM1 composition and sources" by Vecchi et al.

Figure S1: map of site location

Figure S2: Mass absorption coefficient (MAC in m^2/g) derived for this campaign by comparing EC concentrations (by TOT analysis) and b_{abs} (by polar photometry) measured on the same filters.

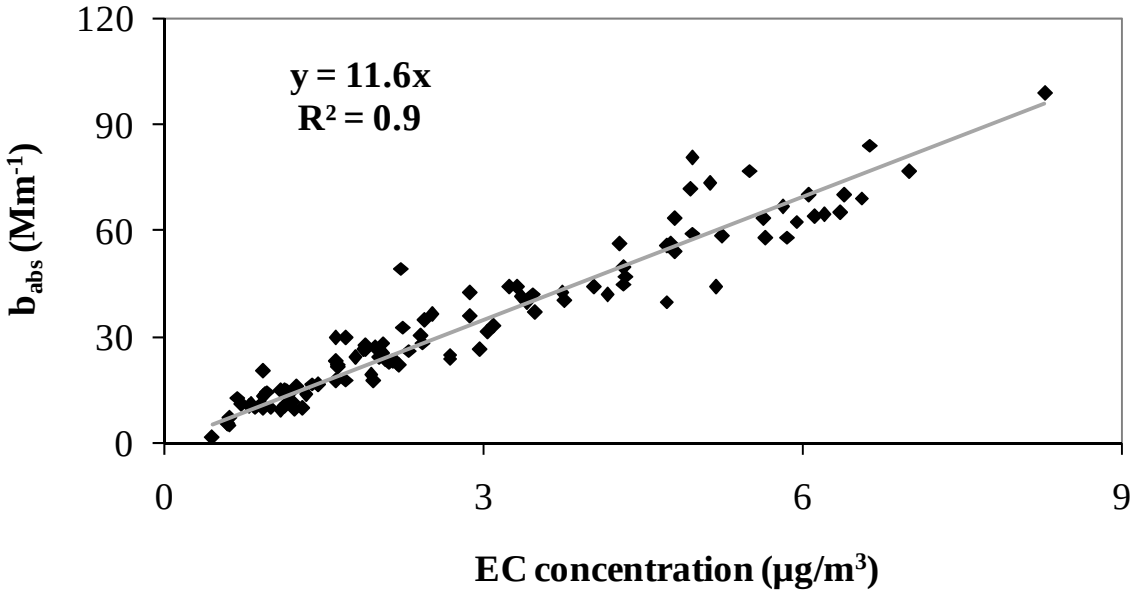

Figure S3: ammonium nitrate concentration (in μg/m^3) recorded in PM10 in Milan during a previous campaign carried out in wintertime 2007. Number concentration (in particles/m^3) for the size bin 0.45-0.50 μm is also reported thus showing that ammonium nitrate was mainly found in the accumulation mode (as expected).

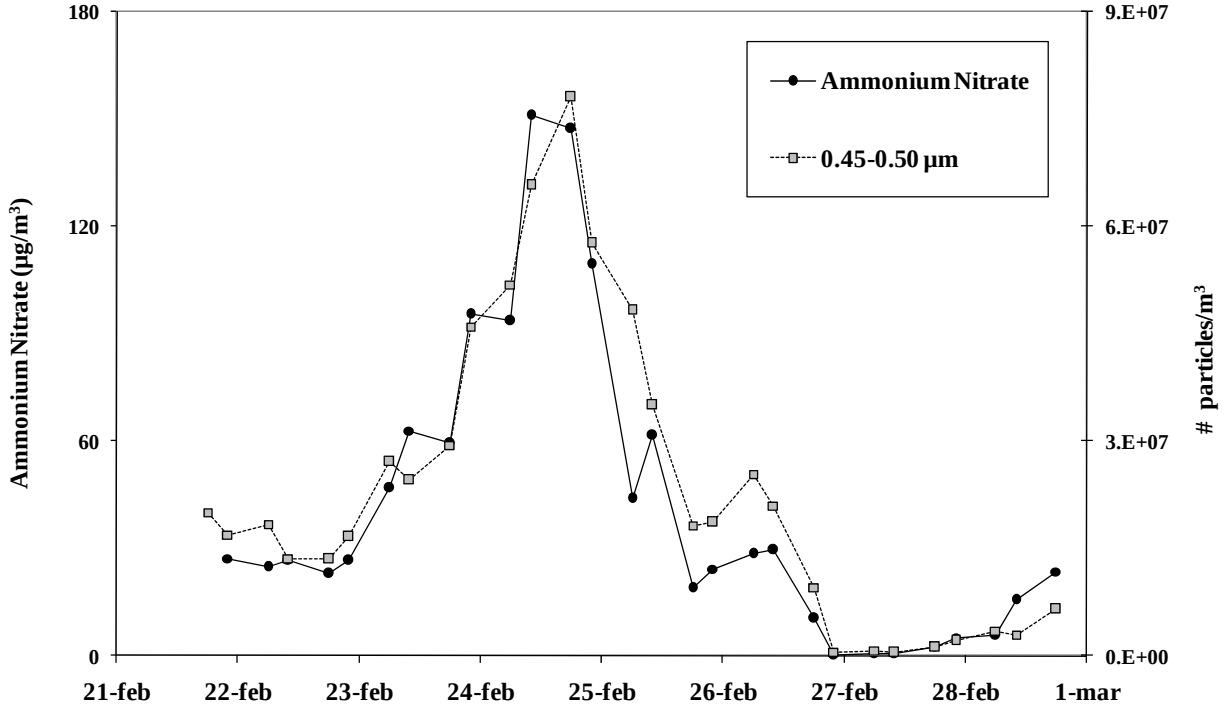

Figure S4: temporal patterns for aerosol light extinction ($b_{ext,aer}$ in Mm^{-1}) and for each aerosol component calculated using the IMPROVE-like algorithm with tailored coefficients.

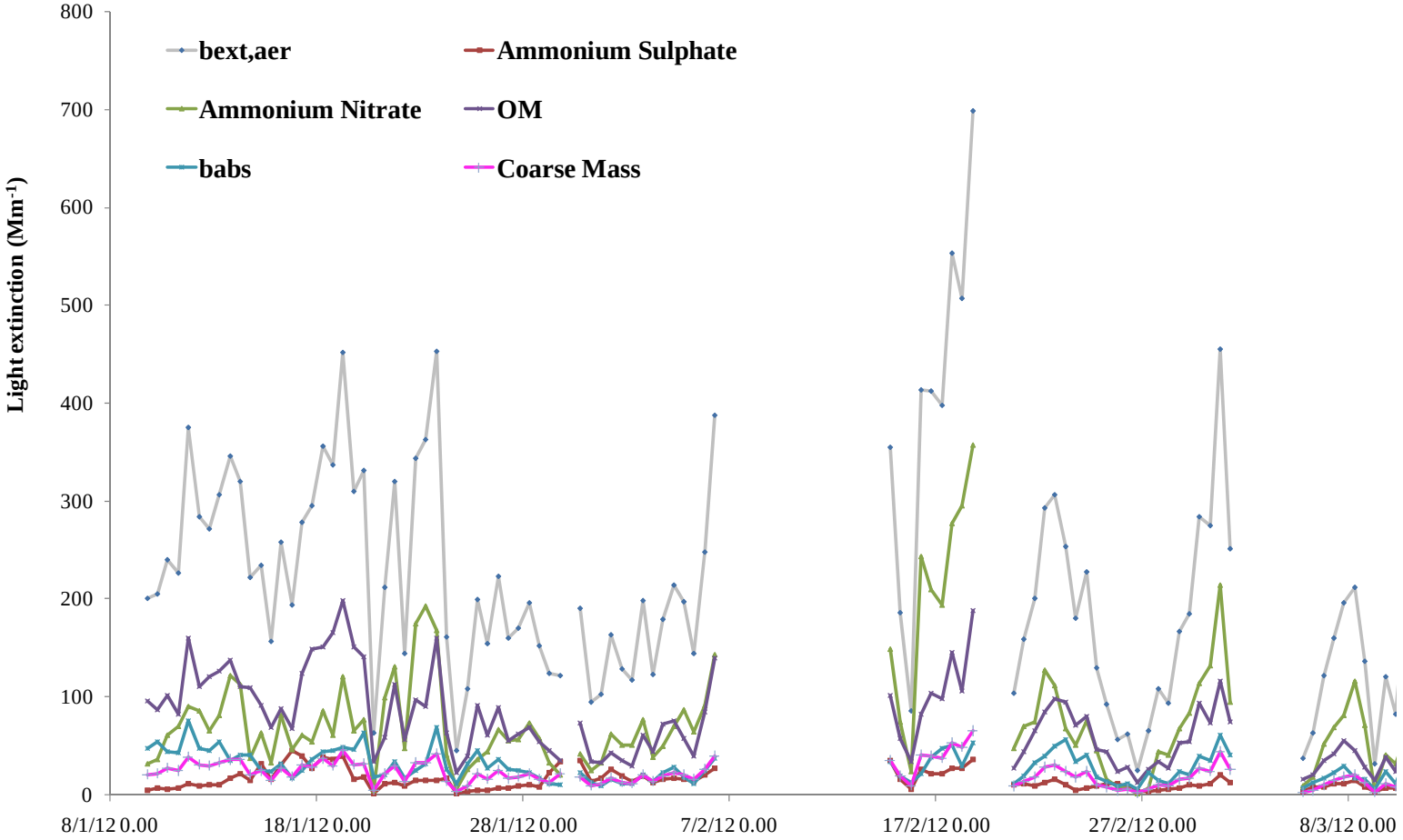

Table S1: basic statistics on chemical species (in ng/m^3) detected in PM1

All samples

	Si	**S**	**Cl**	**K**	**Ca**	**Ti**	**V**	**Cr**	**Mn**	**Fe**	**Ni**	**Cu**	**Zn**	**Br**	**Pb**	**EC**	**OC**	**Nitrate**	**Sulphate**	**Ammonium**	**Levoglucosan**
mean	60	737	286	364	26	6	4	5	7	72	3	8	59	11	25	2917	7455	11591	2272	4537	522
median	56	645	175	320	22	6	4	5	6	58	3	6	46	8	20	2237	6486	9617	1823	4049	379
10°perc	29	298	42	131	11	4	3	4	3	24	2	2	18	5	10	916	2897	3385	762	1655	122
90°perc	86	1346	716	672	45	8	6	6	13	141	4	14	117	19	42	5815	14044	21934	4309	8228	1107

Daytime samples (07-16 LT)

	Si	**S**	**Cl**	**K**	**Ca**	**Ti**	**V**	**Cr**	**Mn**	**Fe**	**Ni**	**Cu**	**Zn**	**Br**	**Pb**	**EC**	**OC**	**Nitrate**	**Sulphate**	**Ammonium**	**Levoglucosan**
mean	66	760	267	339	32	6	4	5	8	72	3	7	62	9	24	2799	6988	11440	2312	4540	398
median	59	639	187	294	29	6	4	5	6	61	3	7	50	8	19	2251	6037	10036	1864	4194	320
10°perc	35	307	55	133	13	4	3	4	4	28	2	2	21	5	9	933	2917	3591	1025	1931	112
90°perc	93	1373	706	613	48	8	5	6	13	140	4	12	139	16	41	5780	12105	18909	4195	7512	716

Nighttime samples (19-04 LT)

	Si	**S**	**Cl**	**K**	**Ca**	**Ti**	**V**	**Cr**	**Mn**	**Fe**	**Ni**	**Cu**	**Zn**	**Br**	**Pb**	**EC**	**OC**	**Nitrate**	**Sulphate**	**Ammonium**	**Levoglucosan**
mean	54	714	302	388	20	6	4	5	7	72	3	9	56	13	27	3032	7913	11736	2233	4535	634
median	52	674	160	350	17	5	4	5	5	56	3	6	45	9	21	2210	6994	9305	1771	3814	484
10°perc	27	278	38	131	9	4	3	4	3	24	2	3	17	5	10	829	3071	3179	731	1517	135
90°perc	82	1282	809	705	36	7	6	6	13	153	4	16	115	23	42	5727	15058	24548	4783	8395	1274

Table S2: source contribution estimates

	Sulphate	**Traffic**	**Pb-rich**	**Wood burning**	**Nitrate**	**Fine dust**	**Industry**
All data	7.1 µg/m^3 **18.9%**	4.5 µg/m^3 **12.0%**	2.1 µg/m^3 **5.5%**	4.8 µg/m^3 **12.8%**	14.0 µg/m^3 **37.4%**	1.6 µg/m^3 **4.3%**	3.4 µg/m^3 **9.0%**
Daytime data	7.2 µg/m^3 **19.9%**	4.5 µg/m^3 **12.4%**	2.0 µg/m^3 **5.4%**	3.4 µg/m^3 **9.5%**	13.7 µg/m^3 **38.0%**	1.8 µg/m^3 **5.1%**	3.5 µg/m^3 **9.7%**
Nighttime data	7.0 µg/m^3 **18.0%**	4.5 µg/m^3 **11.7%**	2.2 µg/m^3 **5.6%**	6.2 µg/m^3 **15.9%**	14.3 µg/m^3 **36.9%**	1.4 µg/m^3 **3.6%**	3.2 µg/m^3 **8.3%**